

ζ -potential characterization of collagen and bovine serum albumin modified silica nanoparticles: a comparative study

William J. Znidarsic · I.-Wei Chen ·
V. Prasad Shastri

Received: 10 June 2008 / Accepted: 8 September 2008 / Published online: 8 October 2008
© Springer Science+Business Media, LLC 2008

Abstract In this study, bovine serum albumin (BSA) and collagen (COLL) were adsorbed independent of one another, onto the surface of silica nanoparticles (SNPs) at pH's where the ζ -potential of the proteins were equal in magnitude, but opposite to the SNP surface to ascertain the differences in surface coverage and conformation in the adsorbed layer. In both systems, increasing the concentration of free protein resulted in an increase in protein surface coverage and ζ values, with ζ values approaching that of native protein at high surface coverage. However, a lower critical charge reversal concentration range was measured for COLL relative to BSA (COLL: 0–25 $\mu\text{g}/\text{mL}$, BSA: 25–90 $\mu\text{g}/\text{mL}$). Additionally, a considerable difference in ζ for adsorbed protein versus free protein was observed. These results when interpreted in terms of the theory of Ottewill and Watanabe indicate a higher Gibbs energy of association for COLL versus BSA on SNP surfaces, accompanied by perturbation in protein structure.

Introduction

In order to harness the potential of stem- and progenitor-cell-based therapies in regenerative medicine, strategies for controlling the cellular microenvironment, especially with regard to presentation of molecular and structural cues

need to be developed. Key to this strategy is the ability to present information at length scales that are compatible with chemical and mechanical signal transduction pathways. To date, the focus has been in composing a cellular microenvironment with spatial and temporal fidelity in soluble (and tethered) biomolecular signals (peptides, proteins, and growth factors). Among the many tools in nature's "tool box," the physical attributes of the cellular microenvironment represent a very key element in controlling cell fate and function and has been minimally explored. We recently demonstrated in two seminal studies that nano-scale physical cues are powerful mediators of mammalian cell function [1, 2]. Using an assembly of silica nanoparticles (SNPs) as the source of the nano-scale physical cues, we have shown that cell shape, cytoskeletal organization [2] and gene expression at the mRNA level can be influenced in terminally differentiated cells and progenitor cells [1]. Based on these findings, we believe that SNPs represent a unique paradigm for influencing cell function. SNP are also advantageous from the stand point of controlling the length-scale and local density of information, as they can be synthesized in various sizes with narrow distribution [3] and be readily functionalized [4]. In order to further explore this paradigm of using SNP assemblies to influence cell function, a strategy to modify and present information on SNP needs to be developed. Borrowing from nature, we envision the assembly of information on collagen (COLL) frameworks using protein and polysaccharide mediators. The first step is to gain an understanding of how the dynamics of protein adsorption are influenced when adsorption occurs on surfaces whose dimensions are comparable to that of the protein.

Towards this end, we studied the adsorption of serum albumin and COLL, the two most abundant proteins in plasma and extra-cellular matrix (ECM), respectively, on

W. J. Znidarsic · I.-W. Chen · V. P. Shastri
Department of Materials Science, University of Pennsylvania,
Philadelphia, PA 19104, USA

V. P. Shastri (✉)
Department of Biomedical Engineering, Vanderbilt University,
5824 Stevenson Center, Nashville, TN 37235, USA
e-mail: prasad.shastri@gmail.com;
prasad.shastri@vanderbilt.edu

Table 1 Representative properties of BSA and type-I collagen

	Collagen [5, 6]	BSA [25]
Dimensions (nm ³)	300 × 1.5 × 1.5	11.6 × 2.7 × 2.7
Molar mass (g mol ⁻¹)	300,000	67,000
Conformation	Triple-helical	α-helical

600 nm SNP, a size that is comparable to the length of COLL (300 nm) [5, 6]. Specifically, the adsorption of bovine serum albumin (BSA) and type-I collagen independently of one another, onto the surface of mono-dispersed SNPs was studied.

The proteins chosen for this study differ not only in their size, but also in their physicochemical properties and tertiary structure (Table 1) and physiological roles. Serum albumin is produced in the liver and is the most abundant protein in mammalian plasma, constituting approximately 60% of plasma protein. In contrast, collagen is generally secreted by a number of cell types and forms the ECM of numerous biological tissues (e.g., skin, bone, and tendon). Collagen is the most abundant protein in the extracellular matrix (ECM) space of the mammalian body, constituting approximately 25–30% of total body protein. Unlike serum albumin which has an α-helical structure and is considered a “soft-protein,” type I collagen molecule in contrast contains three helical polypeptide chains arranged to form a triple helical conformation that imparts rigidity [6]. The ability of collagen to form the ECM is partly attributed to collagen being non-soluble under physiological conditions. This is manifested in an end-to-end aggregation of the rigid-rod collagen molecules to form collagen fibrils. While albumin and collagen differ in origin and structure, similarities exist. For example, both are composed of hydrophobic and hydrophilic amino acids, making them amphipathic molecules. Furthermore, like serum albumin, aqueous solutions of individual type I collagen molecules are stable under acidic conditions and can be used for in vitro adsorption studies. Besides these considerations, the choice of these two proteins was also dictated by the vast body of literature on the adsorption behavior of these proteins on negatively charged surfaces such as modified silicon [7] and poly(styrene sulfonate) [8, 9]. These studies have shown that the adsorption of proteins at a solid–liquid interface can occur in a differential manner and be accompanied by conformational changes in the adsorbed proteins [8, 10]. Specifically, it has been observed that collagen is preferentially adsorbed onto negatively charged surfaces from a binary solution of collagen and serum albumin. This preferential adsorption of collagen has been attributed to a lower degree of electrostatic repulsion at the substrate surface for collagen relative to serum albumin. This highlights the critical role of material surface characteristics in the interrogation of the

biological environment. Towards the development of biomimetic nanoparticles the two objectives of this study were (1) to investigate how solution concentration affects proteins surface coverage and (2) to map the deviations of ζ of the protein-coated substrate as a function of pH from native protein, in order to discern any potential perturbations in protein structure upon adsorption.

Materials and methods

Chemicals

Ethanol, ammonium hydroxide, and HPLC grade water was purchased from Fisher Scientific. Type-I collagen was obtained from BD Sciences as a solution and was diluted as per the manufacturers instructions to the appropriate concentration prior to use. BSA was obtained as a crystalline solid from Sigma Chemicals (St. Louis, MO, USA) and used without any further purification. Tetraethylorthosilicate (TEOS), fluorescein isothiocyanate (FITC) labeled BSA, and type-I collagen were purchased from Sigma-Aldrich as crystalline solids and dissolve in water immediately prior to use.

Synthesis of SNP

Monodispersed SNP was synthesized using the Stöber process [3]. A TEOS/ethanol solution was prepared by taking 5.83 g of TEOS then adjusting the final volume to 50 mL using ethanol. Next, an NH₄OH/H₂O/ethanol solution was prepared by mixing 14.4 g of water with 11.7 g of ammonium hydroxide then adjusting the final volume to 50 mL using ethanol. The TEOS/ethanol and NH₄OH/H₂O/ethanol solutions were then mixed and stirred for 20 h to yield colloidal SNP. The colloidal SNP was washed three times with deionized water to remove any excess reactant using centrifugation. In the last centrifugation step, the final volume of the colloidal SNP was adjusted to 100 mL using deionized water. To determine the particle concentration of the colloid, 1 mL was dried on a glass slide and weighed using a mass balance.

Characterization of SNP

Size and surface charge (ζ) characterization

The SNP was characterized using a Malvern Instruments Ltd, Zeta-sizer 3000, equipped with a laser light scattering setup. Samples were prepared by placing a drop of colloidal SNP into a cuvette containing 2 mL of deionized water at pH 4.5 and the data were collected in the size and zeta mode using software provide by the manufacturer.

Scanning electron microscopy

The size and surface morphology of the SNP was verified using scanning electron microscopy. Samples were prepared by placing a drop of colloidal SNP onto an aluminum stub covered with conductive carbon tape. After solvent evaporation in a drying oven at 70 °C, the stub was sputter coated with Au/Pd prior to imaging using a JEOL 6300F FEG HRSEM operated at an accelerating voltage of 5 kV. The images were captured using the software provided by the instrument manufacturer.

Protein adsorption on SNP

For both collagen and BSA, a sample set was prepared by adding 600 µg/mL of protein stock solution (pH 5.5) to 15 mL conical tubes. The volume of stock solution added to each sample in the set was such that following dilution to 4 mL, the protein concentrations were 0, 100, 280, 360, and 600 µg/mL. For each sample in the set, half of the volume (2 mL) was then transferred to a separate 15 mL conical tube containing 6 mL of colloidal SNP (concentration of particles = 14 mg/mL, pH 5.5) resulting in a set of protein–colloid mixtures with concentrations of protein at 0, 25, 70, 90, and 150 µg/mL. The protein–colloid mixtures were then adjusted to pH 4.5, as at this pH ζ of free BSA and free collagen is positive and equivalent in magnitude, while ζ of the native SNP was negative. The mixture was then stirred for 20 h. Following mixing, the protein-coated colloidal SNP was separated from the protein solution using centrifugation, washed three times with deionized water to remove excess protein in the solutions. In the last centrifugation step, each sample was concentrated to a final volume of 3 mL.

Characterization of protein-coating on SNP

To verify that the presence of a protein layer on the SNP, fluorescence of SNP solutions was measured using a fluorescence spectrophotometer and the SNP were imaged using a laser scanning confocal microscope. The fluorescence intensity of 1.5 µL of the colloidal SNP coated at a concentration of 150 µg/mL protein was measured for FITC fluorescence using a Nanodrop ND-3300 spectrophotometer equipped with a blue LED with peak emission at 470 ± 10 nm (Nanodrop, Inc.). Nanoparticle emission was measured at the 520 nm which is the emission maxima for FITC. Confocal images of the protein-coated particles were obtained using a Carl Zeiss LSM 510 Meta confocal microscope equipped with a 30-mW Argon laser emitting at 488 nm, with a 63× oil immersion objective. An aliquot of 1.5 µL of the SNP sample was mounted on a slide with 50% glycerol and the images of the SNP on the plane of the

glass surface in the standard FITC emission channel (Carl Zeiss, Inc.) were captured and processed using the Zeiss software.

Estimations of protein surface coverage

For each sample, estimates of protein surface coverage were calculated by dividing estimates of adsorbed protein by estimates of particle surface area. Quantitative colorimetric determination using the micro-BCA Assay was used for estimations of adsorbed protein [11, 12]. The micro-BCA assay is a very sensitive assay for quantification of protein in the nanogram range and is widely used in biological research. The assay was validated prior to analysis using BSA standards of known concentration. First, 50 µL of each sample was transferred to a separate 1.5 mL conical tube and then diluted to 1 mL using deionized water. The samples were then incubated in micro-BCA assay reagent following the standard test-tube protocol outlined in the micro-BCA instruction manual. For each sample, following the incubation period, the particles were centrifuged and the supernatant was removed, added to a cuvette, and the optical density measured using a UV–VIS spectrophotometer. In the presence of protein, the reagent forms a water soluble complex resulting in strong absorbance at 562 nm that is directly related to the amount of protein. To quantify the mass of protein in each sample, the optical absorbance for each sample was compared with a plot of optical absorbance for a set of protein standards prepared using the protocol outlined in the Pierce instruction manual. The standard plot was linear in the concentration range of 0.5–20 µg/mL. The particle surface area was estimated using the mass of particles in each sample (measured using a micro-balance), the particle size (estimated from light scattering), and a density of 2.2 g/cm³ (as for macroscopic silica substrates) [4].

ζ -Measurements

ζ -measurements as a function of pH for free BSA, free collagen, native SNP, BSA-coated SNP, and collagen-coated SNP were made using a Malvern Instruments Ltd, Zetasizer 3000. For each sample, pH was varied between measurements using ammonium hydroxide and acetic acid.

Results

Light scattering and SEM of SNP

Light scattering revealed that the nominal size of the SNP was 600 nm (± 30 nm) with a polydispersity index of approximately 0.1 (data not shown). SEM micrograph of a

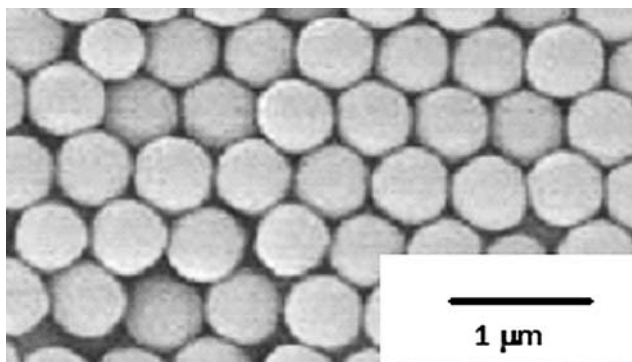


Fig. 1 SEM of native silica nanoparticles

typical SNP preparation (Fig. 1) confirms that the SNP are indeed monodispersed and their size is consistent with that obtained from light scattering measurements. Furthermore, the surfaces of the SNP appear smooth at the resolution of imaging.

Fluorescence spectrophotometry and laser confocal microscopy of protein-coated SNP

Fluorescence spectrophotometry and laser scanning confocal microscopy of colloidal SNP coated with 150 μg/mL

solution of COLL and BSA is shown in Fig. 2. For both BSA/SNP and collagen/SNP, fluorescent spectrophotometry shows fluorescent emission at a wavelength characteristic of the FITC-conjugated protein (Fig. 2a). The corresponding laser scanning confocal microscopy images reveal that the fluorescent protein molecules are concentrated at discrete points that have a diameter approximately that of the SNP (600 nm) (Fig. 2b and c).

Estimations of protein surface coverage

The adsorption conditions (i.e., protein concentration), the resulting measurements of protein surface coverage for BSA-coated SNP (BSA/SNP) and collagen-coated SNP (Collagen/SNP) are shown in Table 2. For both BSA/SNP and collagen/SNP, surface coverage increased with an increase in protein concentration and varied from approximately 0–0.4 μg/cm² when the protein concentration was in the range of 0–150 μg/mL. Values of surface coverage for collagen ranged from 0.08 to 0.44 μg/cm² and that for BSA ranged from 0.12 to 0.4 μg/cm² and falls within the range of those previously reported for adsorption of protein in this concentration range [13].

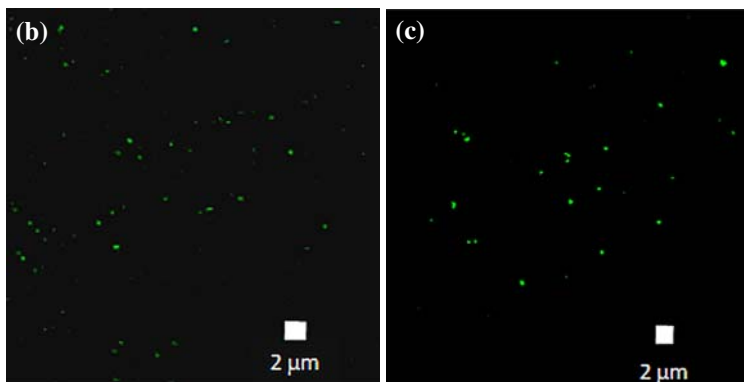
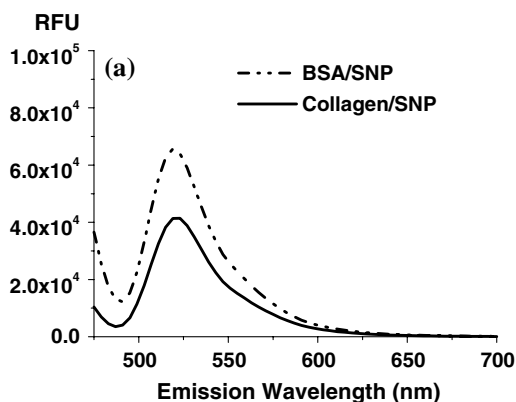


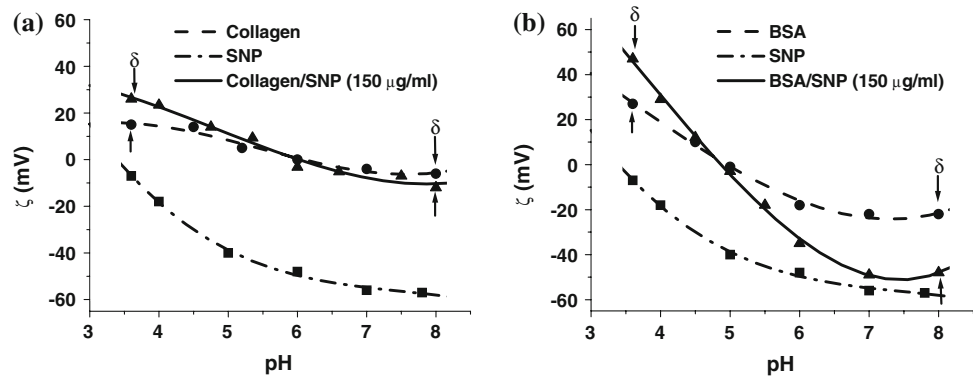
Fig. 2 a Fluorescence emission spectra of SNP coated with FITC–collagen and FITC–BSA, laser scanning confocal microscopy of b FITC–collagen-coated silica nanoparticles (collagen/SNP) and c FITC–BSA-coated silica nanoparticles (BSA/SNP)

Table 2 Characterization of collagen and BSA-coated silica nanoparticles at the pH of adsorption (pH 4.5): ‘c’—concentration of protein added, ‘Γ’—resulting surface coverage, and ‘ζ’—zeta potential

c (μg/mL)	Collagen/SNP		BSA/SNP	
	Γ (μg/cm ²)	ζ at pH 4.5 (mV)	Γ (μg/cm ²)	ζ at pH 4.5 (mV)
0	0	−29 ± 3	0	−29 ± 3
25	0.08 ± 0.02	10 ± 3	0.12 ± 0.03	−22 ± 3
70	0.12 ± 0.03	18 ± 2	–	–
90	0.14 ± 0.02	19 ± 2	0.16 ± 0.02	3 ± 4
150	0.44 ± 0.02	19 ± 2	0.4 ± 0.03	15 ± 4

The values reported are an average of at least three different samples

Fig. 3 Zeta potential (ζ) following washing and pH adjustments for silica nanoparticles coated with **a** collagen at a high concentration (collagen/SNP 150 $\mu\text{g}/\text{mL}$) and **b** BSA at a high concentration (BSA/SNP 150 $\mu\text{g}/\text{mL}$). ζ -values for native silica nanoparticles (SNP), free collagen and free BSA are also included for comparison



ζ -Measurements of BSA/SNP and COLL/SNP

The ζ -measurements at the pH of adsorption (pH 4.5) for BSA/SNP and Collagen/SNP are shown in Table 2. Consistent with the theory of Ottewill and Watanabe [14], ζ of the SNP surface increased with increase in concentration of free collagen and free BSA and approached ζ of the free protein. Adsorption of both proteins resulted in a charge reversal of the SNP surface. However, adsorption of collagen resulted in a lower charge reversal concentration (CRC) relative to BSA (between 0 and 25 $\mu\text{g}/\text{mL}$ for collagen and between 25 and 90 $\mu\text{g}/\text{mL}$ for BSA).

The ζ -measurements as a function of pH for native SNP, free collagen, and collagen/SNP (coated at 150 $\mu\text{g}/\text{mL}$); and free BSA and BSA/SNP (coated at 150 $\mu\text{g}/\text{mL}$) are shown in Fig. 3a and b, respectively. These data points were arbitrarily fitted to a fourth-order polynomial by regression analysis (as is typically done in the literature) [14]. Based on this curve fitting, an IEP of ~ 3.5 for native SNP, ~ 5 for free BSA, and around 5.5 for free collagen was estimated and was found to be consistent with reported values [4, 15, 16]. Interestingly, for both BSA/SNP and collagen/SNP, the IEP of the coated particles (around 5 and 5.5 for BSA/SNP and collagen/SNP, respectively), was found to be approximately that of the free protein an observation previously reported for BSA/SNP [16]. Furthermore, for both BSA/SNP and collagen/SNP below the IEP, ζ for the coated particles is more positive than ζ of the free protein; and above the IEP ζ of the coated particles is more negative than ζ of the free protein (the deviations are labeled as ' δ '). Therefore, the charge on the adsorbed protein is apparently higher than the free protein when plotted in reference to the IEP. A similar observation has been reported in the literature for the adsorption of BSA on to negative charged polystyrene particles [16].

Discussion

It is well established that the surface of a biomaterial is forever altered upon exposure to biological medium due

to the dynamic adsorption of proteins at the solid–liquid interface [13]. Not surprisingly, the composition and the structure of the protein layer affect cellular events at that interface [17, 18]. Furthermore, in the case of proteins such as collagen that possess super-structure, multiple layers of adsorbed proteins with reversible adsorption kinetics have been observed [5]. In all these studies, the adsorption conditions have been shown to be an important variable [19]. For albumin, in vitro studies have shown that adsorption can occur even when the protein and substrate surface have the same charge [8, 9, 20]. Adsorption despite electrostatic repulsion is attributed to increase in entropy resulting from perturbations in the relatively “soft” α -helical structure of serum albumin [20]. Since collagen has a triple helical structure that is considered relatively “rigid,” the increase in entropy resulting from structural perturbations are expected to be minimal. As a result, studies involving competitive adsorption of collagen and serum albumin to silica surfaces attribute preferential adsorption to a lower degree of electrostatic repulsion at the substrate surface for collagen relative to serum albumin [7, 21]. To eliminate the contribution of electrostatic repulsion adsorption studies were carried at pH's where the ζ -potential of the proteins were the same to ensure that the electrostatic repulsion at the substrate surface was similar for each protein. The presence of a robust layer of BSA and COLL on the SNP was verified using fluorescence spectroscopy (Fig. 2a), confocal microscopy (Fig. 2b and c), and quantitative protein analysis (Table 2). In view of this, the implications of the trends observed in the ζ as a function of pH may be explained in part by the theory of Ottewill and Watanabe [14].

Theory

The theory of Ottewill and Watanabe predicts changes in ζ of a substrate surface due to adsorption of free molecules at concentration ' c ' to be given by a Langmuir expression [22, 23].

$$\Delta\zeta_{\text{Sub}} = A \frac{kc}{(1+kc)} N(ze),$$

where A is a constant dependent on substrate and solvent properties, k is the association constant, N is the number of adsorption sites on the substrate, z is the charge on the absorbing molecules, and e is the electronic charge.

Since N can be considered proportional to the hydrodynamic radius (b) of the adsorbing molecules ($N \sim b$) the expression can be written as

$$\Delta\zeta_{\text{Sub}} = A' \frac{kc}{(1+kc)} \frac{(ze)}{b}$$

and assuming the potential of the free molecule $(ze)/b$ is equal to ζ of the free molecule (ζ_{free})

$$\Delta\zeta_{\text{Sub}} = A' \frac{kc}{(1+kc)} \zeta_{\text{free}}$$

Therefore, it can be shown that the change in ζ of the substrate with concentration ‘ c ’ is given by

$$\frac{d\zeta_{\text{Sub}}}{dc} = A' \frac{k}{1+2kc+k^2c^2} \zeta_{\text{free}},$$

therefore, the following expression can be used to compare adsorption of free molecule A and free molecule B at equivalent concentration

$$\frac{d\zeta_{\text{Sub}}/dc^A}{d\zeta_{\text{Sub}}/dc^B} = \frac{k_A[1+2k_Bc+k_B^2c^2] \zeta_{\text{free}}^A}{k_B[1+2k_Ac+k_A^2c^2] \zeta_{\text{free}}^B}$$

and when $\zeta_{\text{free}}^A = \zeta_{\text{free}}^B$

$$\frac{d\zeta/dc^A}{d\zeta/dc^B} = \frac{k_A[1+2k_Bc+k_Bc^2]}{k_B[1+2k_Ac+k_Ac^2]}$$

So that as c goes to zero, i.e., at low concentrations

$$\frac{d\zeta/dc^A}{d\zeta/dc^B} = \frac{k_A}{k_B}$$

Since the Gibbs energy of association per mole at temperature T (ΔG°) is given by

$$\Delta G^\circ = -RT \ln k$$

For molecule A relative to molecule B, this theory predicts that comparisons in ΔG° can be made by comparing $d\zeta_{\text{Sub}}/dc$ at low concentrations.

However, while this theory assumes no change in ζ for adsorbed protein relative to free protein, i.e., $\zeta_{\text{ads}} - \zeta_{\text{free}} = 0$, several studies have reported that considerable changes occur and attribute this effect to structural perturbations that change the size, i.e., $b_{\text{ads}} - b_{\text{free}} > 0$, and/or charge, i.e., $ze_{\text{ads}} - ze_{\text{free}} > 0$ of the protein molecules [8–10, 16, 20, 24, 25].

In this study, two proteins BSA and collagen with completely different size and physicochemical characteristics

were studied (Table 1). To eliminate the effect of charge–charge interaction induced changes in protein–surface affinity and synergistic and cooperative effects of binary protein systems, BSA and collagen were adsorbed separately to the surface of mono-dispersed SNPs and the electrostatic repulsion between the substrate surface and the protein molecules was set to be similar by adjusting the pH at the initial adsorption conditions such that ζ of free BSA and free collagen was initially cationic and comparable in magnitude while ζ of the SNP surface was initially anionic. An increase in concentration of the free protein resulted in an increase in surface coverage of the SNP surface that in turn caused ζ of the SNP surface to increase, reverse charge, and approach ζ of the free protein. Comparisons of critical charge reversal concentrations (CRC) revealed a lower CRC for collagen relative to BSA (between 0 and 25 $\mu\text{g}/\text{mL}$ for collagen and between 25 and 90 $\mu\text{g}/\text{mL}$ for BSA) and therefore a larger initial $d\zeta/dc$. When interpreted in terms of the theory of Ottewill and Watanabe, the higher $d\zeta/dc$ for collagen indicates a higher Gibbs energy of association [14, 23]. However, as stated earlier this theory assumes no change in ζ for adsorbed protein relative to free protein. However, in this study, for both BSA and collagen, changes in pH yielded changes in ζ for adsorbed protein relative to free protein. Such a discrepancy between ζ of the adsorbed and free protein as a function of pH has been reported for BSA when adsorbed on flat macroscopic substrates and has been attributed structural perturbations that change the size and/or charge of the protein molecules [18, 26]. The additional finding that such discrepancies occur even in collagen—a relatively “rigid” molecule with a robust triple helical structure, suggests that changes to the tertiary structure of proteins upon adsorption to nano-scale interfaces is highly likely and should be taken into consideration in the engineering of nano-scale biomimetic systems.

Acknowledgements This work was supported in part by a GANN fellowship to WJZ, a research grant from the Nanotechnology Institute (NTI) via Ben Franklin Technology Partners of Northeast Pennsylvania to VPS and IWC and the Vanderbilt Institute of Chemical Biology (VICB). The authors thank Ashwath Jayagopal for help with the confocal images of the protein-coated SNP and Dr. Christopher Pino for helpful suggestions.

References

1. Lipski AM, Jaquiere C, Choi H, Eberli D, Stevens M, Martin I et al (2007) Adv Mater 19:553. doi:10.1002/adma.200502617
2. Lipski AM, Pino CJ, Haselton F, Chen I-W, Shastri VP (2008) Biomaterials 29(28):3836. doi:10.1016/j.biomaterials.2008.06.002
3. Stöber W, Fink A, Bohn E (1968) J Colloid Interface Sci 26:62. doi:10.1016/0021-9797(68)90272-5

4. Iler RK (1979) The chemistry of silica-solubility, polymerization, colloidal and surface properties, and biochemistry. Wiley & Sons, Chichester
5. Deyme M, Baszkin A, Proust JE, Perez E, Boissonnade MM (1986) *J Biomed Mater Res* 20:951. doi:[10.1002/jbm.820200710](https://doi.org/10.1002/jbm.820200710)
6. Kucharz EJ (1992) The collagens: biochemistry and pathophysiology. Springer-Verlag, Berlin
7. Ying P, Yu Y, Jin G, Tao Z (2003) *Colloid Surf B Biointerf* 32:1. doi:[10.1016/S0927-7765\(02\)00133-9](https://doi.org/10.1016/S0927-7765(02)00133-9)
8. Norde W, Lyklema J (1978) *J Colloid Interface Sci* 66:257. doi:[10.1016/0021-9797\(78\)90303-X](https://doi.org/10.1016/0021-9797(78)90303-X)
9. Norde W, Lyklema J (1978) *J Colloid Interface Sci* 66:266. doi:[10.1016/0021-9797\(78\)90304-1](https://doi.org/10.1016/0021-9797(78)90304-1)
10. Norde W, Lyklema J (1978) *J Colloid Interface Sci* 66:285. doi:[10.1016/0021-9797\(78\)90306-5](https://doi.org/10.1016/0021-9797(78)90306-5)
11. Micro BCA Protein Assay Kit Instructions. Thermo Scientific Life Science Research Products
12. Krajewski A, Piancastelli A, Malavolti R (1998) *Biomaterials* 19:637. doi:[10.1016/S0142-9612\(97\)00153-1](https://doi.org/10.1016/S0142-9612(97)00153-1)
13. Horbett TA (1993) *Cardiovasc Pathol* 2:S137. doi:[10.1016/1054-8807\(93\)90054-6](https://doi.org/10.1016/1054-8807(93)90054-6)
14. Ottewill RH, Watanabe A (1960) *Colloid Polym Sci* 170:132. doi:[10.1007/BF01525172](https://doi.org/10.1007/BF01525172)
15. Barbani N, Lazzeri L, Cristallini C, Cascone MG, Polacco G, Pizzirani G (1999) *J Appl Polym Sci* 72:971. doi:[10.1002/\(SICI\)1097-4628\(19990516\)72:7<971::AID-APP13>3.0.CO;2-N](https://doi.org/10.1002/(SICI)1097-4628(19990516)72:7<971::AID-APP13>3.0.CO;2-N)
16. Norde W, Lyklema J (1978) *J Colloid Interface Sci* 66:277. doi:[10.1016/0021-9797\(78\)90305-3](https://doi.org/10.1016/0021-9797(78)90305-3)
17. Keresztes Z, Rouxhet PG, Remacle C, Dupont-Gillain C (2006) *J Biomed Mater Res A* 76:223. doi:[10.1002/jbm.a.30472](https://doi.org/10.1002/jbm.a.30472)
18. Knowles GC, McKeown M, Sodek J, McCulloch CA (1991) *J Cell Sci* 98(Pt 4):551
19. Sutoh K, Noda H (1974) *Biopolymers* 13:2461. doi:[10.1002/bip.1974.360131206](https://doi.org/10.1002/bip.1974.360131206)
20. Norde W, Lyklema J (1978) *J Colloid Interface Sci* 66:295. doi:[10.1016/0021-9797\(78\)90307-7](https://doi.org/10.1016/0021-9797(78)90307-7)
21. Ying P, Jin G, Tao Z (2004) *Colloid Surf B Biointerf* 33:259. doi:[10.1016/j.colsurfb.2003.10.015](https://doi.org/10.1016/j.colsurfb.2003.10.015)
22. Hunter RJ (1981) Zeta potential in colloidal science. Academic Press, New York
23. Taboada P, Mosquera V, Ruso JM, Sarmiento F, Jones MN (2000) *Langmuir* 16:6795. doi:[10.1021/la9912904](https://doi.org/10.1021/la9912904)
24. Norde W, Anusiem ACI (1992) *Colloid Surf* 66:73. doi:[10.1016/0166-6622\(92\)80122-I](https://doi.org/10.1016/0166-6622(92)80122-I)
25. Norde W, Favier JP (1992) *Colloid Surf* 64:87. doi:[10.1016/0166-6622\(92\)80164-W](https://doi.org/10.1016/0166-6622(92)80164-W)
26. Pamula E, De Cupereb V, Dufrêneb YF, Rouxhet PG (2004) *J Colloid Interface Sci* 271:80. doi:[10.1016/j.jcis.2003.11.012](https://doi.org/10.1016/j.jcis.2003.11.012)